Journal of Optoelectronics and Advanced Materials Vol. 5, No. 4, December 2003, p. 801 - 816

Section 5a. OPTOELECTRONIC MATERIALS
Invited Paper

THE EFFECT OF THE ELECTRON IRRADIATION ON THE STRUCTURAL AND ELECTRICAL PROPERTIES OF A^{II}-B^{VI} THIN POLYCRYSTALLINE FILMS

S. Antohe*, L. Ion, V. A. Antohe

Faculty of Physics, University of Bucharest, P.O. Box MG-11, Bucharest-Magurele, 077125 - Romania

The electrical properties of the non-irradiated and electron irradiated structures, containing polycrystalline thin films of CdS and CdSe, sandwiched between two gold electrodes, were investigated. The thin films of CdS and CdSe were obtained through thermal-vacuum evaporation on the glass substrate at temperature of 220 °C. After the investigation of their structure by X-ray diffraction (XRD), the samples were subjected to two sessions of irradiation with 7 MeV and 6 MeV accelerated electrons to different fluences. The current-voltage characteristics, recorded at temperatures in the range 150÷400 K, showed that the Ohm's law is followed at low-applied voltages, in both non-irradiated and irradiated CdS and CdSe layers. In the range of high-applied voltages, the dominant conduction mechanism is the space-charge-limited-current (SCLC), controlled by different type of trap distribution, placed in the band gap of the semiconducting film. An analysis in the frame of SCLC theory allowed to get the parameters that characterize the trap distribution and the changes induced by electron irradiation.

(Received July 16, 2003; accepted August 21, 2003)

Keywords: Polycrystalline layers, CdS, CdSe, Electron irradiation

1. Introduction

The A^{II} - B^{VI} semiconductor compounds, particularly CdS, CdSe, CdTe, are of great interest because they are potential candidates in many practical applications like solar cells, optical detectors, dosimeters of ionized radiation, field-effect transistors and optoelectronic devices. For example, the heterojunctions, based on CdS or CdSe thin layers [1-3], are very promising structures for solar cells because of suitable band gap, optical absorption and good stability of the materials. The development of low cost solar cells depends on the exploitation of thin films and, thus, CdS, CdSe or CdTe thin films obtained under various experimental conditions, require extensive electrical characterization. Despite of the considerable amount of work, which has been done on the structural and electrical properties of these films [4-10], only a few studies on the influence of the ionizing radiations on their electrical properties have been carried out [11-15]. This paper presents the results related to the effect of electron irradiation on the dark conductivity of polycrystalline CdS and CdSe thin films.

2. Experimental procedures

The sandwich structures like Au/CdS/Au and Au/CdSe/Au respectively, were prepared by the following procedure. A gold film having the shape of a strip of 8 mm length, 2 mm width and 300 nm thickness, was initially deposited on the substrate which was a glass plate maintained at 220 °C during

* Corresponding author: s_antohe@yahoo.com; santohe@solid.fizica.unibuc.ro

the deposition of the semiconducting thin film. A 25 μm layer of CdS and 24 μm layer of CdSe, respectively, were then deposited on the gold electrode. The powder was vacuum sublimated at a pressure of 10^{-5} Torr, from a quartz container heated at 1100 °C for CdS and 750 °C, for CdSe, respectively. Finally, an other gold strip, with the same dimensions like the back contact was deposited on the top of semiconducting film, in a perpendicular direction with respect to the first one. To improve the stability and the ohmicity of the contacts, the cells were heat treated in air at 250 °C, for 30 minutes [8-11].

The structure of the samples was investigated by X-ray diffraction (XRD), using a θ-2θ XRD diffractometer and CuK_α radiation (λ = 1.54178 Å). A graphite monochromator, placed before the NaI scintillation counter, was used. The experimental geometry corresponded to an instrumental FWHM of $\Delta k = 4.9 \times 10^{-4}$ Å^{-1} (in units of $k = 2 \sin\theta/\lambda$), as determined with a standard α-quartz single crystal.

The samples were irradiated at room temperature in two sessions with 7 MeV electrons at the fluences of: 4×10^{15} electrons/cm^2 and 6×10^{15} electrons/cm^2 for CdS and with 6 MeV accelerated electrons and at the fluences of 2×10^{15} electrons/cm^2 and 4×10^{15} electrons/cm^2, respectively, for the CdSe films.

Before and after each irradiation session, the current-voltage characteristics (I-U) in the range of 150÷400 K have been measured, on the samples introduced in a metallic cryostat to a pressure below 10^{-3} Torr. A copper-constantan thermocouple monitored the sample temperature. The I-U characteristics under dc bias were measured using a stabilized power supply in conjunction with a Philips X-Y recorder.

3. Experimental results and discussions

3.1. Structure

Fig. 1 shows the experimental XRD pattern of a CdSe sample. It indicates a mixture of hexagonal-close-packed (h.c.p.) and face-centered-cubic (f.c.c.) phases, which is usual for the systems that present a normal h.c.p. and/or a f.c.c. structure. In the case of CdSe, the h.c.p. structure is the normal one in the system, while the f.c.c. structure can be described simply as the result of the segregation of the stacking-faults developed in the films during the growth process (superstructure formed on the h.c.p. normal phase). The energy necessary to produce such defects is very low and this explains the presence of the mixture of two phases in almost all systems with close-packed structures. The assessment that the f.c.c. phase is a superstructure formed on the h.c.p. phase, is supported by the relationship existing between the a_h, c_h parameters of the h.c.p structure (two layer periodicity) and the a_c parameter of the f.c.c packing (periodicity of three (111) atom layers).

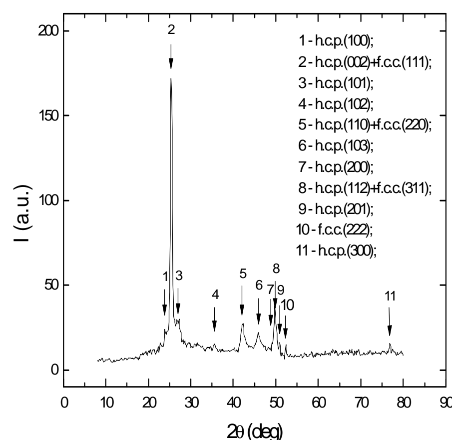

Fig. 1. X-ray diffraction pattern of CdSe thin film.

The dominant h.c.p. phase is mostly (00l) oriented in the growth direction. This relationship reads, for data in Table 1:

$$\text{Calculated} \begin{cases} a_c^{(1)} = a_h\sqrt{2} = 6.076\,\text{Å} \\ a_c^{(2)} = c_h\sqrt{3}/2 = 6.088\,\text{Å} \end{cases} \text{vs. } a_c = 6.079\text{ Å (measured value)} \quad (1)$$

The dominant h.c.p. phase is mostly (00l) oriented in the growth direction. The measured lattice parameters are indicated in Table 1. For the h.c.p. phase a_h coincides with the ideal value ($a_h^0 = 4.299$ Å) within the experimental precision, while c_h is increased by 0.28% by reference to the ideal value ($c_h^0 = 7.010$ Å).

The size of coherent zones D_{eff} and local lattice distortions $<\varepsilon^2>$, as determined from linewidths, are also indicated in Table 1. D_{eff} is larger and $<\varepsilon^2>$ smaller for the f.c.c. phase, hinting to a good crystallization state. The h.c.p. phase is more disordered, presumably due to residual faults.

Table 1 Structural data for phases present in CdSe samples.

Phase	Lattice parameters (Å)	c_h/a_h	$D_{eff}^{(001)}$ (Å)	$<\varepsilon^2>^{1/2}\cdot 10^3$
h.c.p.	a_h=4.296 c_h=7.030	1.636	652	5.3
f.c.c.	a_c=6.079	-	886	1.6

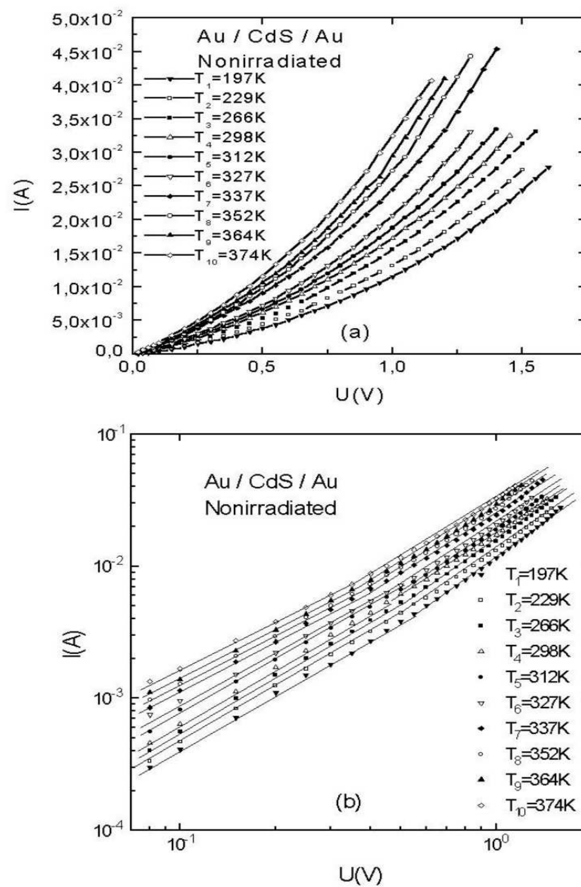

Fig. 2. The I-U characteristics of nonirradiated Au/CdS/Au cells for different temperatures: a) in linear scale; b) in logarithmic scale.

3.2. Electrical properties

3.2.1. Au/CdS/Au structures

3.2.1.1. The I - U characteristics before irradiation

The dark current - voltage characteristics of the Au/CdS/Au cells at 10 temperatures ranging from 197 to 374 K are shown in Fig. 2(a).

The characteristics are completely symmetrical with respect to the polarity of applied voltage. The detailed information about the transport mechanism through the CdS layer may be obtained from I - U characteristics analysis at different tempe-ratures. That is why in Fig. 2(b), the I - U characteristics are shown in a logarithmic plot.

There are two distinct regions in these characteristics: at low voltages the slopes of the logI vs. logU plots are approximately equal to unity (1.18 - 1.37), while at higher voltages, above a well - defined transition voltage U_X, the slopes are approximately equal to two (exactly ranging from 1.7 to 2.14). These plots are typical of ohmic conduction for voltages below U_X and of space charge limited conductivity (SCLC) at voltages above U_X. This is a common feature for the most inorganic [6,7] and organic [14,15] layers, with low mobility and high resistivity. At low voltages there is an ohmic conduction described by Ohm's law:

$$j = qn_0 \mu \frac{U}{d} \tag{2}$$

where: j is the current density, q the electronic charge, n_0 is the concentration of thermally - generated free electrons in the conduction band (CB) at thermal equilibrium, μ is the electron mobility, U is the applied voltage and d is the thickness of CdS film. The concentration of the free electrons of thermal equilibrium is given by:

$$n_0 = N_c \exp\left[-\left(E_c - E_{F_0}\right)/KT\right] \tag{3}$$

where: N_c is the effective density of states in CB of the grains, $E_c - E_{F_0}$ is the separation of the equilibrium Fermi level from CB edge, k is the Boltzmann constant, and T is the absolute temperature. The mobility μ from Eq. (2), it is also a function of temperature. The temperature dependence of the mobility in the polycrystalline thin films was intensively studied in the case of coplanar structures [4,5, 8-10]. Here we have polycrystalline CdS films in a sandwich structure. The cross - sectional views of CdS thin films, [12] revealed a columnar structure that grew perpendicular to the glass substrate if the glass temperature was higher than 200 °C. As a result, in these structures the transport mechanism will be dominant across the crystallites, and this differs from that which takes place in plane (in a direction parallel to the substrate).

Now the electrical properties of the polycrystalline films will be dependent on the certain intracrystalline defects like stacking faults [9]. The effects of stacking faults on the electrical properties will be considered in the cross - plane direction, that is, in a direction perpendicular to the substrate (parallel to the applied electric field in a sandwich cell). The effect of the grain boundaries is minimised in this direction due to the growth process of the grains in thin films [16] and stacking faults generally occur in the *c* plane (or basal plane) of cadmium sulphide. Since our films are highly oriented [11,12] with the *c* axis perpendicular to the glass substrate, it is in the cross - plane direction that these intracrystalline planar defects manifest their major influence on the electrical properties of the CdS layers. CdS is shown to have a low stacking fault energy [17], allowing for the easy formation of such faults during deposition, but also the stress due to difference in thermal expansion between the film and substrate may induce severe faulting by plastic deformation.

Kazmerski et al. [1] developed a model which accounts for the effect on the electrical properties due to the presence of stacking faults in cadmium sulphide, treating the fault as a potential barrier. The band structure of their barrier model is represented as that of hexagonal crystal broken

intermittently by the potentials associated with the stacking faults. In their model the resistivity of sufficiently faulted films is given by:

$$\rho = \rho_b \exp\left(q\Phi_{SF} / kT\right) \tag{4}$$

where ρ is the effective cross - plane resistivity and $q\Phi_{SF}$ is the stacking fault barrier potential. The bulk factor ρ_b was expressed as $\rho = C_{SF}\rho_{crystal}$ where $\rho_{crystal}$ is that part of the resistivity independent of stacking faults, and C_{SF} is a constant which depends on the stacking - fault density being equal to unity if no faults are present and greater than unity if faulting has occurred. According to this model we consider that the mobility of the faulted films (prepared at 220 °C substrate temperature) may be represented by:

$$\mu = \mu_0 \exp\left(-E_{SF} / NT\right) \tag{5}$$

where E_{SF} is the stacking - fault barrier potential and μ_0 is the mobility in the bulk of unfaulted crystallites. Introducing the Eqs. (3) and (5) in Eq. (2) the current density in the ohmic region becomes:

$$j = q\mu_0 N_c \exp\left[-\left(E_c - E_{F_0} + E_{SF}\right)/KT\right]\frac{U}{d} \tag{6}$$

The plot of $ln(I_\Omega/U)$ versus $10^3/T$, for $U = 0.1$ V is shown in Fig. 3(A). I_Ω is the current in the ohmic region, being the current density multiplied by the effective area S, of the structures. There are two straight lines with different slopes. In the range of low temperatures, the electron concentration is essentially independent of temperature, and the activation energy of conductivity could be related to the activation energy of mobility in the other words to the stacking - fault barrier potential E_{SF}. In these assumption the $\ln\left(I_\Omega / U\right)$ could be written as:

$$\ln\left(\frac{I_\Omega}{U}\right) = \ln\left(\frac{Sq\mu_0 n_0}{d}\right) - \frac{\Delta E_1}{10^3 k}\cdot\frac{10^3}{T} \tag{7}$$

where $\Delta E_1 \cong E_{SF}$. According to the Eq. (7), from the slope of the straight line in the range of low temperature (LT) and taking $10^3K = 8.625 \times 10^{-2}$ eV, results $\Delta E_1 \cong E_{SF} = 0.02\,\text{eV}$, in good agreement with the value obtained by L. L. Kazmerski [1].

In the range of high - temperatures (HT), the thermal excitation of the electrons in the conduction band becomes important and the $\ln(I_\Omega/U)$ can be written

$$\ln\left(\frac{I_\Omega}{U}\right) = \ln\left(\frac{Sq\mu_0 n_0}{d}\right) - \frac{\Delta E_2}{10^3 k}\cdot\frac{10^3}{T} \tag{8}$$

where $\Delta E_2 \cong E_c - E_{F_0}$ according with Eq. (6). From the slope of the straight line, in the range of (HT), results $\Delta E_2 = 0.112\,\text{eV}$, and, therefore, $E_c - E_{F_0} \cong 0.112\,\text{eV}$.

In accord with Eq. (8), by extrapolation $1/T = 0$, in the (HT) range, for $d = 25 \times 10^{-4}$ cm, and $S = 0.04$ cm^2, the product $\mu_0 N_c = 2.17$ cm^{-1}V^{-1}s^{-1} was obtained.

Considering the effective mass of electrons in CdS $m_n^* = 0.2\ m$ [18], the effective density of states in the CB, at 300 K is $N_C = 2.2 \times 10^{18}$ cm^{-3}. With this value of N_c it was obtained: $\mu_0 = 0.094\, cm^2/Vs$; $n_0 = 2.5\times10^{16} cm^{-3}$ and the dark conductivity $\sigma_0 = 3.7\times10^{-4}\Omega^{-1}cm^{-1}$, values in good agreement with these reported by other authors for polycrystalline films of CdS [9,10,18].

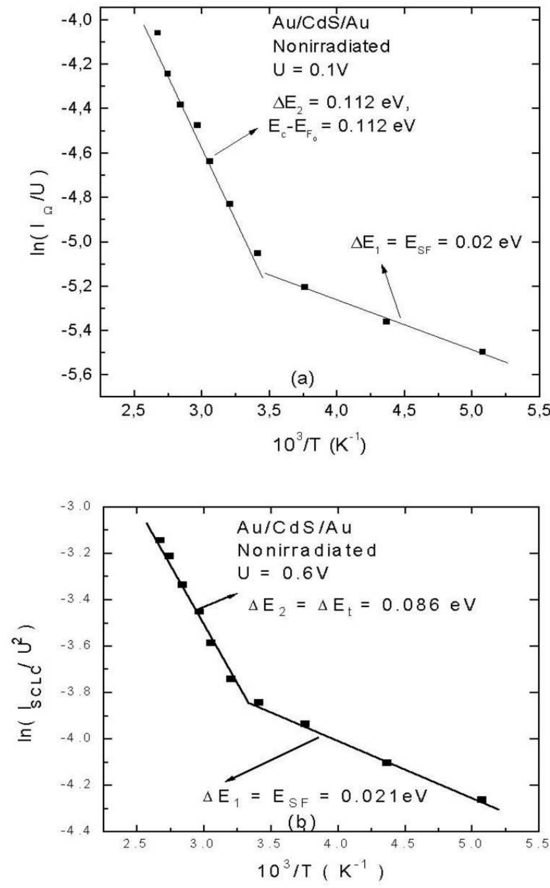

Fig. 3. a) Dependence of ln (I_Ω / U) on the reciprocal temperature $10^3/T$ at U = 0.1 V; b) Dependence of ln (I_{SCLC} / U^2) on reciprocal temperature $10^3/T$ at U = 0.6 V, for the Au/CdS/Au structures.

For applied voltages greater than U_X the slopes of *log I* versus *log U* characteristics in Fig. 2b are in the range of 1.7 to 2.1, which shows that the current is SCLC controlled by a single dominant trap level. For this case, the current density may be expressed by the following equation [14,19]:

$$j_{SCLC} = \frac{9}{8}\varepsilon\mu_0\theta\frac{U^2}{d^3} \tag{9}$$

where in addition to the symbols defined above, ε represents the permitivity and θ is the ratio of the free to trapped carrier density. The ratio θ is given by:

$$\theta = \frac{N_c}{N_t}\exp\left(-\frac{E_c - E_t}{KT}\right) \tag{10}$$

where N_t is the trap density of trapping level situated at the energy E_t below the CB edge. With Eq. (10), the current density in the SCLC region becomes:

$$j_{SCLC} = \frac{9}{8}\varepsilon\mu_0\frac{N_c}{N_t}\exp\left(-\frac{E_c - E_t}{KT}\right)\frac{U^2}{d^3} \tag{11}$$

and from the plot of $\ln\left(I_{SCLC}/U^2\right)$ versus $(1/T)$, the E_c-E_t and N_t values may be obtained. Fig. 3(B) shows the dependence of $\ln\left(I_{SCLC}/U^2\right)$ versus $\left(10^3/T\right)$ for the voltage U = 0.6 V. $I_{SCLC} = S \times j_{SCLC}$ is the current in the SCLC region. Again two straight lines with different slopes were obtained. In the range of (LT) the slope of the line leads to the value E_{SF} = 0.021 eV, closely equal to that resulting from the ohmic region in the same range of temperature. In the range of (HT), from the slope of the straight line and from its intercept with the current axis, according to the Eq. (11), the values E_c-E_t = 0.086 eV and $N_t = 8.9 \times 10^{15}$ cm^{-3} were obtained, respectively. To obtain these values, we considered $\varepsilon = 1.02 \times 10^{-8}$ F/cm [9] and $\mu_0 N_c = 2.07 \times 10^{17}$ $cm^{-1}V^{-1}S^{-1}$ (as above determined). The values of the quantities (μ_0, n_0, σ_0, E_{SF}, $E_c - E_{F_0}$, E_c-E_t, N_t) are in good agreement with those reported before for evaporated CdS films [9,10].

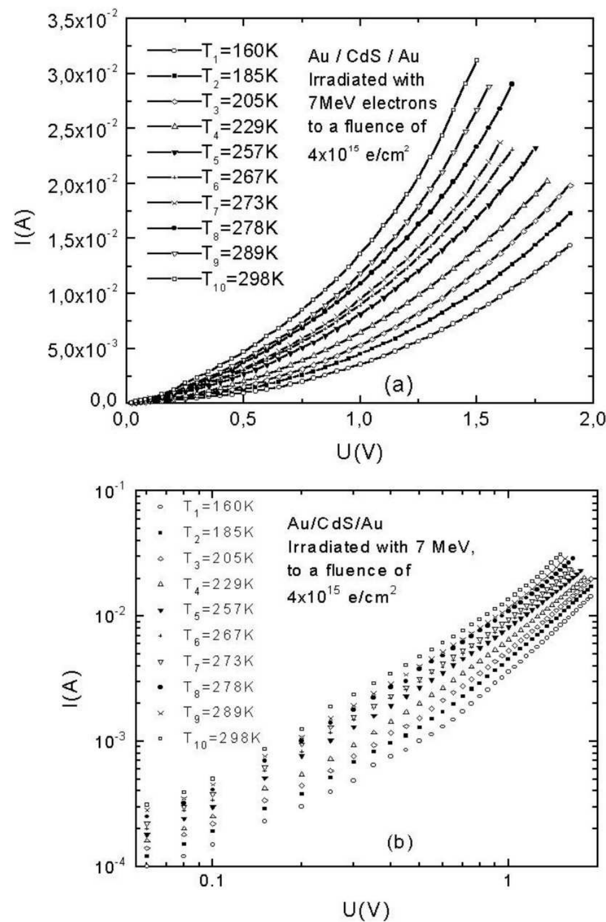

Fig. 4.The I-U characteristics for the Au/CdS/Au cells irradiated with 7 MeV electrons to a fluence of 4×10^{15} e/cm^2, for different temperatures: (A) in linear scale; (B) in logarithmic scale.

3.2.1.2 The I - U characteristics after irradiation

The current-voltage characteristics of the Au/CdS/Au cells, after the first session of irradiation with 7 MeV electrons to a fluence of 4×10^{15} e/cm^2 are shown in a linear and logarithmic plot in Fig. 4a, b. The I - U characteristics in logarithmic plot Fig. 4b, suggest that again two distinct conduction mechanism are present. At low voltages (0.05 - 0.5 V) the slopes of the *log I* versus *log U* are around unity (0.98 – 1.2), suggesting the presence of an ohmic conduction. Following the treatment used in the case of the low voltages range of I - U characteristics of nonirradiated cells we

obtained from, $\ln(I_\Omega U) = f(10^3/T)$ plot, Fig. 5(A), the values: E_{SF} = 0.025 eV and E_c-E_{F0} = 0.0876 eV.

The value of E_{SF} is a little larger than that obtained in the case of nonirradiated cells suggesting that the irradiation determines the increase of the barriers associate with the stacking - faults. On the other hand in the range of high - voltage the *log I - log U* plot, Fig. 4b don't show a set of straight - lines. In the range of 0.5 - 2 V, the plot $\ln(I/U) = f(U)$ gives a set of straight - lines suggesting the presence of a space - charge - limited - current in the case of an uniform traps distribution in the band - gap of the CdS layer (Fig. 5b).

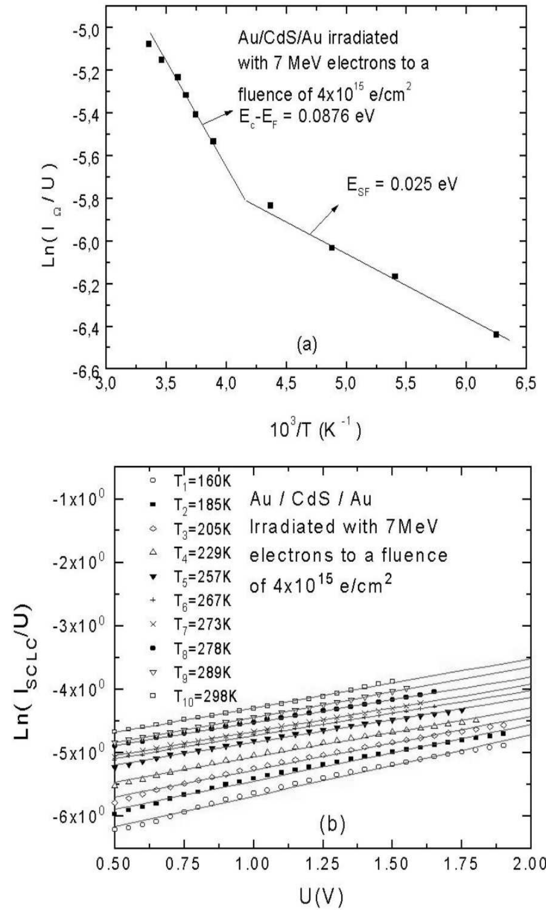

Fig. 5. The dependence of: a) ln (I_Ω / U) = f(10^3/T) at U = 0.1 V; b) ln (I_{SCLC} / U) = f(U), for the Au/CdS/Au cells irradiated with 7 MeV electrons to a fluence of 4×10^{15} e/cm^2.

The uniform trap distribution may be described by:

$$\rho(E) = \frac{dN_t}{dE} \tag{12}$$

where N_t is the total density of traps distributed in the energetic band dE = E_1-E_2, placed inside the band - gap of semiconductor. According to Rose's treatment [20] the current density of SCLC is described by:

$$j_{SCLC} = \frac{9}{8} q\mu_0 n_0 \frac{U}{d} \exp\left(\frac{\varepsilon U}{qd^2 KT\rho(E)}\right) \tag{13}$$

The plot of $\ln(I/U) = f(U)$ in the range of 0.5 - 2 V, Fig. 5b, gives a set of straight - lines. The slope of a line, from this set, gives the value of *ρ(E)* and its intercept on the *ln(I/U)* axis gives the possibility to find n_0 according to the equation:

$$\ln\left(\frac{I_{SCLC}}{U}\right) = \ln\left(\frac{9}{8}S\frac{q\mu_0 n_0}{d}\right) + \frac{\varepsilon}{qd^2 KT\rho(E)}U \tag{14}$$

Fitting our experimental data with the eq. (14), and considering for μ_0 and N_c the above determined values, we obtained for *ρ(E)* and n_0 the average values 6.43 × 10^{17} $cm^{-3}eV^{-1}$ and 1.42 × 10^{16} cm^{-3}, respectively. Also, here, we observe a very weak temperature dependence of the equilibrium Fermi level, and its average value is equal to that obtained in the case of nonirradiated layers. A situation like this one was reported in the case of polycrystalline thin films of CdTe [4]. This behavior, after the first session of irradiation, shows that the irradiation with electrons determines some changes on the transport of the charge carriers through the thin layers. These changes could be associated with the effect of the irradiation which increases the barriers associated to stacking - faults and increases the number of the traps in the band - gap of the semiconductor. These defects could be the vacancies of Cd induced by irradiation.

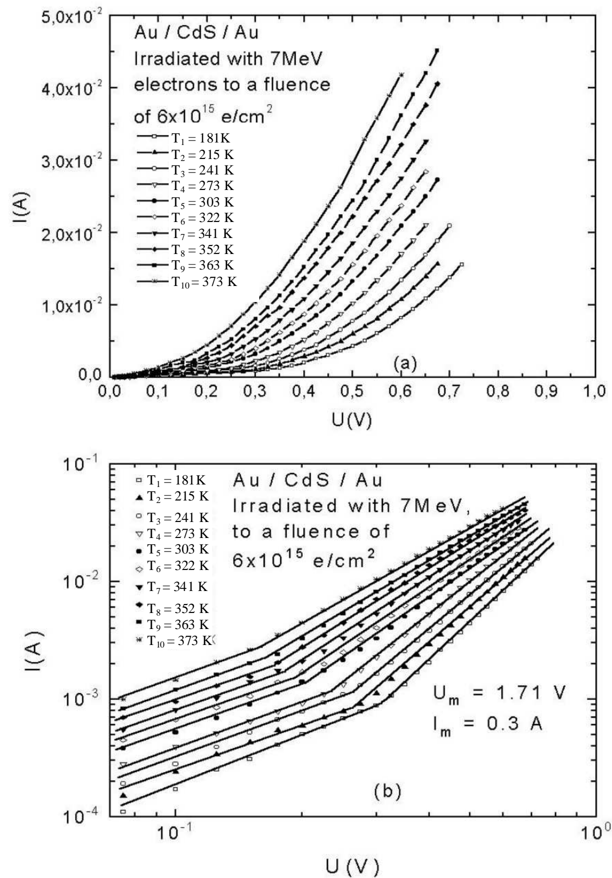

Fig. 6. The I-U characteristics for the Au/CdS/Au cells irradiated with 7 MeV electrons to a fluence of 6 × 10^{15} e/cm^2 for different temperatures: a) in linear scale; b) in logarithmic scale.

After the second session of irradiation with 7 MeV electrons to a fluence of 6 × 10^{15} e/cm^2 the current - voltage characteristic was measured and the plot in linear and logarithmic scale are shown in Fig. 6a, and 6b, respectively. Again there are two distinct regions in the logarithmic plot of *I-U* characteristics Fig. 6b. At low - voltages (0.05 - 0.2 V) the slopes of the straight lines being

approximately equal to 1 while at higher - voltages (U > 0.2 V), the slopes are larger than 2, varying in the range of (3.5 - 2.1) when the temperature increases from 181 K to 373 K. This type of behavior may be accounted for in terms of ohmic conduction at low - voltages and space - charge limited conduction in presence of an exponential trap distribution at higher – voltages [6,7,15].

Following the treatment used in the case of the low - voltages range of I-U characteristics of the previous cases, above analysed, we obtain from the $\ln(I_\Omega / U) = f(10^3 / T)$ plot at U = 0.1 V (Fig. 7) the values: $E_{SF} = 0.03$ eV and $E_c - E_{F_0} = 0.112$ eV.

The value of E_{SF} increases again after the second session of irradiation suggesting that the process responsible for the increase of E_{SF} during the first session of irradiation further continues along the second irradiation .

Now, new is the fact that in the range of high-voltages appears a SCLC current in presence of an exponential trap distribution.

According to Lampert [13] the space-charge-limited J-U characteristics for an n-type semiconductor with an exponential distribution of trapping levels is given by:

$$J_{CLSS} = q\mu N_c \left(\frac{\varepsilon}{qN_t}\right)^{\gamma} \frac{U^{\gamma+1}}{d^{2\gamma+1}} \tag{15}$$

where, in addition to the symbols defined above, N_t represents the total density of trapping levels in the exponential distribution, and γ is the ratio between a temperature parameter T_c and the ambient temperature T . The exponential trap distribution may by described in terms of T_c as:

$$\rho(E) = \frac{N_t}{kT_c} \exp\left(-\frac{E}{kT_c}\right) \tag{16}$$

where $\rho(E)$ is the trap density per unit energy range at an energy E below the *CB* edge and N_c / kT_c is the value of $\rho(E)$ at the *CB* edge. On the basis of this expression, it may by seen that the plots $\log J_{CLSS}$ versus logU for different temperatures are straight lines having the slopes larger than 2 ($T_c \geq T$) and decreasing when the temperature increases. As a results of this behavior it is clear that the straight lines intersect at a common point. The coordinates of this point are [8,13]:

$$U_m = \frac{N_t q d^2}{\varepsilon};\ j_m = q\mu N_c \frac{U_m}{d} \tag{17}$$

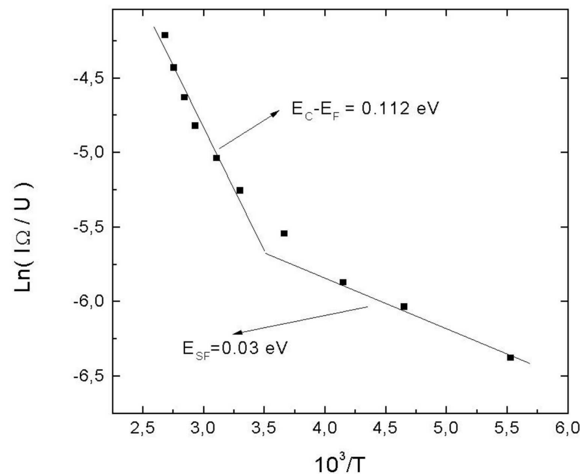

Fig. 7. Dependence of ln (I_Ω / U) on the reciprocal temperature 10^3/T at U = 0.1 V, for the Au/CdS/Au cells irradiated with 7 MeV electrons to a fluence of 6×10^{15} e/cm^2.

It is evident that the experimental curves $logJ_{SCLC} \sim logU$, in the *SCLC* region, Fig. 6b, are straight lines, with different slopes, as predicted by the theory. When the temperature increases from 181 K to 373 K the slopes decrease from 3.4 to 2.1 and then the ratio γ decrease from 2.4 to 1.1. Using the values of γ for the temperatures inserted in Fig. 6b, we obtain the mean value of T_c: $\overline{T}_c \cong 440$ K.

Furthermore, the coordinates of the intersection point of the lines are (U_m = 1.17 V and I_m = 0.3 A), as calculated from the experimental data of the least squares fit. These coordinate values yield $N_t = 1.74 \times 10^{16}$ cm^{-3} and μ = 0.03 cm^2/Vs considering in Eq. (17) $\varepsilon = 1.02 \times 10^{-8}$ F/cm and $N_c = 2.2 \times 10^{18}$ cm^{-3}. Thus, from simple measurements of I-U characteristics at different temperatures, the parameters μ, T_c and N_t have been derived assuming only the well - documented semiconductor constant ε and N_c . These results obtained after the second irradiation suggest that an increase in the irradiation dose to 6×10^{15} e/cm^2 led to a decrease of mobility as a result of increasing of potential barriers associated with stacking faults. On the other hand the increasing in the irradiation dose lead to the appearance of an exponential trap distribution below the CB of CdS layer with an increased total trap concentration. During the irradiation with electrons, both a migration of the defects and impurity atoms (non - stoichiometric atoms Cd or S) and the generation of new vacancies of Cd or S take place in these samples, so that a change in the concentration and distribution of traps could be present.

3.2.2. Au/CdSe/Au structures

The current-voltage characteristics of the cells, before and after the two sessions of irradiation, are nonlinear and completely symmetrical with respect to the polarity of the applied voltage. At low voltages (below about 1 V) the Ohm's law is followed, with a thermally activated conductivity. The temperature dependence of the electrical conductivity is well described by the relation:

$$\sigma(T) = \sigma_1 \, exp\left(-\frac{E_{a1}}{k_B T}\right) + \sigma_2 \, exp\left(-\frac{E_{a2}}{k_B T}\right), \tag{18}$$

as demonstrated by the plot in Fig. 8. The values of the parameters entering eq. (18), as obtained by numerical fit, are indicated for the Au/CdSe/Au cells, in Table 2.

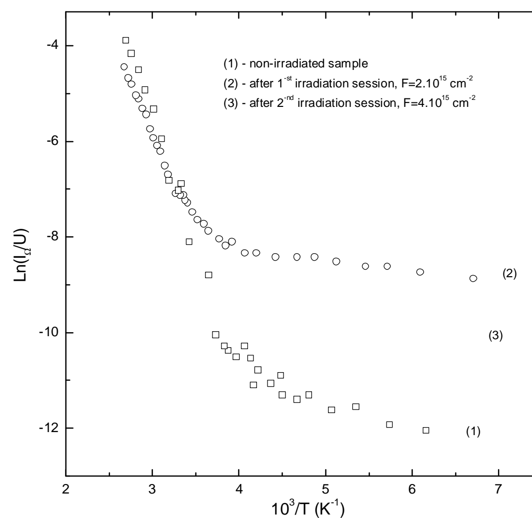

Fig. 8. Dependence of the electrical conductivity on reciprocal temperature, for the non-irradiated sample (1) and after two subsequent irradiation sessions with 7 MeV electrons to the fluences: 2×10^{15} cm^{-2} (2) and 4×10^{15} cm^{-2} (3), respectively.

The results suggest that there are two competing conduction mechanisms. The first term in eq. (18), with larger activation energy and dominating in the high temperature range, corresponds to the conduction band mechanism. The second, dominating at low temperatures, corresponds to the hopping conduction involving the localized states induced by the structural and/or chemical disorder in the band gap. The values of σ_2 and E_{a2} are typical for hopping mechanism. Electron irradiation causes the Fermi level shift towards the conduction band (CB) and an important decrease of the preexponential factor σ_1, i.e. a decrease of the mobility.

Table 2. The parameters describing the electrical properties of the CdSe films and the defect band states.

Conditions	σ_1 ($\Omega^{-1}cm^{-1}$)	$E_{a1}=E_c-E_{F0}$ (eV)	σ_2 ($\Omega^{-1}cm^{-1}$)	E_{a2} (eV)	N_0 ($cm^{-3}eV^{-1}$)	$\|E_0\|$ (eV)	ΔE (eV)
before irradiation	514.17	0.46	4.59×10^{-6}	0.048	1.09×10^{14}	0.41	0.055
after 1^{-st} irradiation	91.44	0.42	8.54×10^{-6}	0.018	3.31×10^{14}	0.41	0.052
after 2^{-nd} irradiation	11.47	0.37	4.69×10^{-6}	0.029	5.74×10^{14}	0.41	0.052

A possible explanation is that the defect states near the Fermi level, induced by irradiation and having the dominant influence on the electrical properties of the films are of donor type. Using the measured values of E_{a1} and E_{a2}, the location of these defect states in the band gap of CdSe can be determined with the following argument. The hopping activation energy E_{a2} is roughly of the order of $|E_0 - E_{F0}|$, where E_0 is the energetic separation between the center of the band of defect states and the bottom of *CB* E_c, and E_{F0} is the equilibrium Fermi level, also measured from E_c [12,22,23]. In the following all energetic values will be considered with respect to E_c, taken as the zero on energy scale (so E_0, $E_{F0} < 0$). If $E_0 > E_{F0}$ (the center of defect band located between the Fermi level and the bottom of CB), states lying near the Fermi level are very rare, their overlap is weak, and consequently, their contribution to the hopping conductivity can be neglected. The main contribution to hopping conduction is due to the electrons activated from the Fermi level into the peak of the density of states, so $E_{a2} = E_0 - E_{F0}$, or equivalently, $E_{a2} = E_{a1} - |E_0|$ (see Fig. 9).

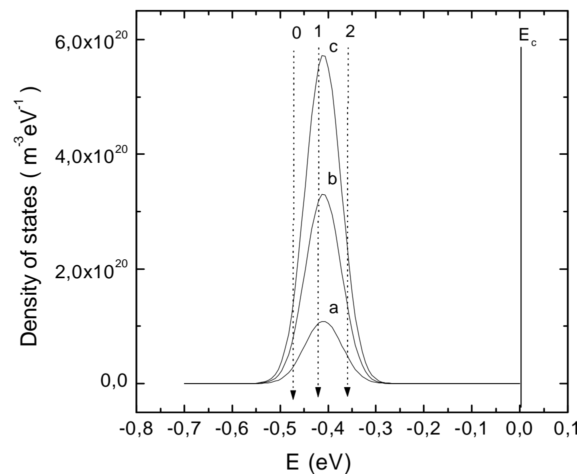

Fig. 9. Model of defect states band in the band gap of CdSe, as suggested by the analysis of the presented transport data. The irradiation influences on the location of the Fermi level (0- non-irradiated, 1-after first and 2- after the second irradiation) and also on the defect states density (a- non -irradiated, b- after first and c- after second irradiation) are indicated.

The same argument holds for the case where $E_0 < E_{F0}$ (the Fermi level located between the center of defect band and the bottom of CB), when the hopping conduction is mainly associated with the motion of the holes over defect states whose energy is close to E_0, and $E_{a2} = E_{F0} - E_0$. This seems to be the case after the second irradiation. Comparing the values of E_{a2} and E_{a1} in Table 2, a value E_0 of about 0.41 eV is obtained. The locations of the defect band and of the Fermi level before and after irradiation are indicated in Fig. 9. The presence of a peak of donor levels located at about 0.4 eV below the conduction band in CdSe films was also reported [20,21,28,29].

At high applied voltages, there is a space-charge-limited conductivity (SCLC), controlled by trap distribution. According to the theory of SCLC current, for a n-type material, the electric field $E(x)$ in the sample is given by the Poisson equation [13]:

$$\begin{aligned} \frac{dE}{dx} &= \frac{e}{\varepsilon_0 \varepsilon_r} \cdot \left(n - n_0 + n_t - n_{t0}\right), \\ E(0) &= 0, \end{aligned} \tag{19}$$

and the current density, constant through the sample, is:

$$j = e\mu_n n(x)E(x) = const. \tag{20}$$

In eq. (19): $n_0 = N_c \, exp\left(\frac{E_{F0} - E_c}{k_B T}\right)$ and n_{t0} are the thermal equilibrium free and trapped carrier density; $n = N_c \, exp\left(\frac{E_F - E_c}{k_B T}\right)$ and n_t denote the same quantities in the non-equilibrium case, when the carrier injection at the contacts become important, $\varepsilon_0 = 8.85\times10^{-12}$ F/m is the vacuum permitivity, $\varepsilon_r = 10$ is the CdSe dielectric constant [14], e is the electron charge, E_{F0} is the equilibrium Fermi level given in Table 2, E_F is the non-equilibrium quasi-Fermi level. Considering the effective mass of electron in CdSe, $m_n = 0.13 \cdot m_0$, the effective density of states in the conduction band was evaluated as $N_c = 2\left(\frac{2\pi \, m_n k_B T}{h^2}\right)^{3/2} = 0.226\times10^{21} T^{3/2}$ m^{-3}. Assuming a set of traps distributed in energy, having as density of states $N_t(E)$, n_t can be written as:

$$n_t = \int_{E_v}^{E_c} \frac{N_t(E)dE}{1 + \frac{1}{2} exp\left(\frac{E - E_F}{k_B T}\right)} = \int_{E_v}^{E_c} \frac{N_t(E)dE}{1 + \frac{n_0}{2n} exp\left(\frac{E - E_{F0}}{k_B T}\right)} \quad . \tag{21}$$

The same expression holds for n_{t0}, with E_F replaced by E_{F0}. Using eqs. (19-21), the electrical field in the sample and, subsequently, the voltage across the sample, corresponding to each value of the current density can be calculated, if the analytical function $N_t(E)$ is known.

In order to interpret the data, we considered, in the case of non-irradiated and irradiated Au/CdSe/Au structures, at high – voltages, that the SCL current is controlled by a Gaussian trap distribution, placed in the vicinity of the Fermi level, described by:

$$N_t(E) = N_0 \, exp\left(-\left(\frac{E - E_0}{\Delta E}\right)^2\right) \tag{22}$$

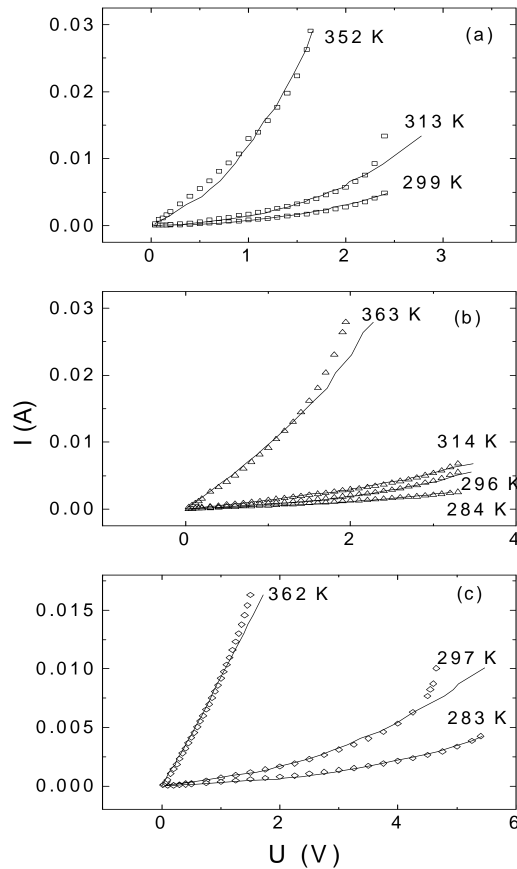

Fig. 10. Current-voltage characteristics at different temperatures, before (a) and after the first (b) and second (c) irradiation sessions. Both the measured values (points) and the best fits (continuous line) obtained as indicated in text are plotted.

A numerical fit procedure was developed for determining the parameters N_0, E_0 and ΔE entering eq. (22). The center of the defect band E_0 was restricted to 0.41 eV below the bottom of the conduction band, following the argument presented above. The I-U characteristics recorded at different temperatures were used (see Fig. 10), the parameters were determined for each of them and the average results are indicated in table 2. For the sake of simplicity only three I-U plots together with the corresponding results of the numerical fit were showed in Fig. 10. For comparison purposes the characteristics recorded at about the same temperatures, for non-irradiated and irradiated structures, have been chosen. As expected, an increase of the defect state density from 1.09×10^{14} $cm^{-3}eV^{-1}$ for the non-irradiated sample to 5.74×10^{14} $cm^{-3}eV^{-1}$ after the second session of irradiation was observed. There is no significant change of the width $\Delta E = 0.11$ eV of the defect band.

4. Discussion about the origin of the defects induced by electron irradiation

We have shown that the investigated films may contain relatively large concentrations of defects such as Cd interstitials and Se vacancies. These are the simplest defects that generate donor states in CdSe. Following irradiation, more complex defects can appear by association of the simpler ones. The samples were irradiated at room temperature, where both vacancies and interstitials may have a large mobility. Some of the defects induced by irradiation disappear by direct recombination

vacancy-interstitial (new defects of type Cd on Se sub-lattice may result). Only those defects stabilized by interaction of one element of the pair (interstitial or vacancy) with another defect (impurity, grain boundary) survive. The creation of complex defects such as vacancy or interstitial clusters involves a much larger free energy, mostly because of the large lattice deformation energy, which those defects imply. The concentration of larger complexes must then be significantly lower than the concentration of vacancies, interstitials and vacancy-interstitial pairs.

Some numeric evaluations, using a super-cell technique, seem to favor the association of the donor level located at 0.40 eV below the conduction band with Se vacancies. There is also some experimental evidence [24-27] favoring the association of the level situated at 0.18 eV below CB to Cd interstitials. These are the simplest donor-like defects in CdSe. This image is also supported by the fact that these defects are produced in large concentrations by electron irradiation.

The maximum energy transmitted by an incident (relativistic, E=0.1÷10 MeV) electron to an atom of the target occupying a lattice site is given by:

$$E_{tm} = 2\frac{m_o}{M}E\left(2+\frac{E}{m_o c^2}\right), \tag{23}$$

where m_0 is the rest electron mass and M is the mass of the target atom. There is a threshold energy E_{th} needed for dislocating the target atom from its lattice site. This energy is of the order of 10-20 eV for most materials (13 eV for Si, 8.6 eV for GaAs). Assuming E_{th} = 10 eV, for a 6 MeV incident electron it results a maximum transmitted energy of 802 eV to a Cd atom and 1142 eV to Se atom. Each dislocated Cd atom can then induce a cascade of 802/(2 × 10) = 40 secondary displacements (57 in the case of Se atoms). Consequently, following an elementary act of collision of incident electron with an atom, a distorted region of the lattice appears with a core containing vacancies and vacancy clusters surrounded by a shell with many interstitials. The irradiation was performed at room temperature and most of these defects disappear after irradiation by direct recombination vacancy-interstitial. Some of the (mobile) interstitials manage to migrate to the surface of grain boundaries where they are stabilized by lattice defects and so interstitials and vacancies survive the recombination process.

5. Conclusions

Using measurements of I-U characteristics for different temperatures in the range (150÷400 K), before and after irradiation, the effect of high-energy electron irradiation on the electrical properties of CdS and CdSe polycrystalline thin films was investigated.

In the range of low-applied voltages in both non-irradiated and irradiated CdS and CdSe films is observed an ohmic conduction. The study of the temperature dependence of the conductivity showed that in the high temperature range the band conduction mechanism dominates. As an effect of irradiation, the Fermi level shifts towards the conduction band, while the mobility of free carriers decreases significantly. In the low temperature range the dominating conduction mechanism is the hopping of the carriers through localized states. In the range of high applied voltages, where the super-ohmic behavior of the I-U characteristics was observed, the space-charge-limited-conductivity (SCLC) has been identified as the dominant conduction mechanism in our samples. The SCL current is controlled by different type of trap distributions placed in the band gap of the semiconductor. The analysis in the frame of SCLC theory offers the possibility to get the parameters characterizing the trap distribution. As expected, the concentration of traps is increased as an effect of electron irradiation. The origin of the defects induced by electron irradiation has been revealed.

References

[1] L. L. Kazmerski, W. B. Berry, C. W. Allen, J. Appl. Phys. **43**, 3515 (1972).
[2] Kazuo Shimizu, Japanese Journal of Applied Physics **4**, 627 (1965).
[3] B. B. Ismail, R. D. Gould, phys. stat. sol.(a), **115**, 237 (1989).
[4] R. D. Gould, B. B. Ismail, Int. J. Electron. **69**, 19-24 (1990).
[5] B. A. Kulp, Phys. Rev. **125**, 1865 (1962).

[6] H. Ohyama, K. Hayama, phys. stat. sol. (a) **142**, K.117 (1994).
[7] I Spânulescu, I. Secareanu, N. Båltåteanu, I. Z. Abdi, T. Khalass, Thin Solid Films **143**, 1 (1986).
[8] V. Ruxandra, S. Antohe, J. Appl. Phys. **84**, 727 (1998).
[9] J. Dresner, F. V. Shallcross, Solid-State Electronics **5**, 205 (1962).
[10] J. Dresner, F. V. Shallcross, J. Appl. Phys. **34**, 2391 (1963); G. G. Rusu, J. Optoelectron. Adv. Mater. **3**(4), 861 (2001).
[11] V. Ruxandra, J. Mater. Sci. Lett. **16**, 1833 (1997)
[12] B. I. Shklovskii, A.L. Efros, in Electronic Properties of Doped Semiconductors (Springer Verlag, Berlin, 1984), pp. 180-191.
[13] M. A. Lampert, P. Mark, Current Injection in Solids (Academic Press, New York, 1970), pp. 33-38.
[14] D. E. Brodie, J. LaCombe, Canadian Journal of Physics **45**, 1353 (1967)
[15] P. Cristea, I. Spânulescu, I. Secåreanu, V. Ruxandra, S. Spânulescu, N. Baltåteanu, Journal of Material Science Letters **12**, 1467 (1993).
[16] S. Antohe, V. Ruxandra, L. Ion, Diana Facâna, T. Strugariu, M. Pavelescu, Romanian Reports in Physics, Vol. 50, Nrs. (7-8-9), 625-633, (1998)
[17] V. Ruxandra, S. Antohe, L. Ion, Delia Doroş, M. Pavelescu, T. Strugariu, Romanian Reports in Physics, Vol. 50, Nrs. (7-8-9), 615-623, (1998)
[18] S. Antohe, V. Ruxandra, L. Ion, Oana Porumb, Romanian Reports in Physics **52**(5-6-7), 467 (2000).
[19] L. Ion, Roxana Schiopu, V. A. Antohe, V. Ruxandra, S. Antohe, Romanian Reports in Physics, **53**(3-8), 451 (2001).
[20] S. Antohe, L. Ion, V. Ruxandra, J. Appl. Phys. **90**(12), 5928 (2001).
[21] V. A. Ambegaokar, B. I. Halperin, J. S. Langer, Phys. Rev. **B4**, 2612 (1971).
[22] B. I. Shklovskii, A. L. Efros, Zh. Eksp. Theor. Fiz. **60**, 867 (1971) (in russian).
[23] B. I. Shklovskii, A. L. Efros, "Electronic Properties of Doped Semiconductors", Springer Verlag, Berlin, 1984.
[24] G. F. J. Garlick, A. F. Gibson, Proc. Phys. Soc. **60**, 574 (1948).
[25] R. H. Haering, E. N. Adams, Phys. Rev. **117**, 451 (1960).
[26] L. Ion, Ph. D. Thesis, University of Bucharest, 2002.
[27] S. Ignatowicz, A. Kobendza, "Semiconducting Thin Films of $A^{II}B^{VI}$ Compounds", PWN-Polish Scientific Publishers, Warszawa-Poland, Ellis Horwood Ltd., Chichester-GB, 1990.
[28] S. Antohe, V. Ruxandra, H. Alexandru, Journal of Crystal Growth, 237-239, 1559-1565, (2002).
[29] S. Antohe, L. Ion, V. A. Antohe, Romanian Journal of Physics, **48**, 511 (2003).